Converting surface plasmon to spatial Airy beam by graded grating on metal surface

X. M. Tang, L. Li, T. Li,* Q. J. Wang, X. J. Zhang, S. N. Zhu, and Y. Y. Zhu

National Laboratory of Solid State Microstructures, School of Physics, College of Engineering and Applied Sciences, Nanjing University, Nanjing 210093, China

**Corresponding author: taoli@nju.edu.cn*

Received April 1, 2013; accepted April 9, 2013;
posted April 15, 2013 (Doc. ID 188055); published May 15, 2013

A well-developed phase modulation method is utilized to design a nanogroove grating for a desired diffraction process, which gives rise to the conversion of a surface plasmon wave to an Airy-like radiation beam. Experiments and simulations revealed the unique characteristics of the generated Airy-like beam, such as nonspreading, self-bending, and self-healing. Our result confirms the validation of the diffraction strategy for beam engineering in conversions and possibly indicates wider applications in broader areas. © 2013 Optical Society of America

OCIS codes: (050.1970) Diffractive optics; (050.6624) Subwavelength structures; (240.6680) Surface plasmons.
http://dx.doi.org/10.1364/OL.38.001733

Surface plasmon polaritons (SPPs) attract great research enthusiasm due to their two-dimensional subwavelength confinement of field at the metal/dielectric surface. It is of scientific interest and potential applications to convert SPP to free space with a desired form by compact micro structures. Since the pioneer work of bulls eye structure [1], plasmonic subwavelength components are widely utilized to tailor the radiation beams to realize collimation [1], focusing [2], concentration [3], holographic vortex [4], and imaging [5]. In our recent work, we have proposed a new method in phase modulation with nonperiodic array for diffractions to generate a plasmon Airy beam and focused totally in a planar dimension [6–8]. It is quite possible to extend this in-plane process to a radiation scheme and the conversion of SPP to a free space beam, which would greatly enrich this phase modulation method in a wider beam engineering area.

Since their first realization in 2007, nondiffraction Airy beams have gained growing attention for their unconventional properties including nondiffracting, self-accelerating, and self-healing [9]. Intense studies have been carried out on their novel [10,11] and fascinating applications [12]. More recently, nonparaxial beams with similar properties with circular and elliptical trajectories [13,14] were proposed and realized. At the same time, a free-space Airy beam convert from SPP is reported by the holographic method via Fourier transformation (FT) [15]. According to the data, the experimental achievements of optical accelerating beams need bulky optical elements such as spatial light modulators for phase modulation and lenses for FT, which take up a great deal of space and would limit the applications in compact microsystems.

In this work, we extended our phase modulation method to convert SPP waves to free space radiation and generate an Airy-like beam by a well-designed groove grating directly. The nonspreading, self-bending, and self-healing properties are demonstrated by experiments and theoretical calculations. Finally, the general significance of our result is further addressed.

The phase modulation method by in-plane diffraction was first introduced in our previous work [6]. Intuitively, this phase modulation method by diffraction can be extended to free space. The schematic design is shown in Fig. 1(a), where parameter b represents the local lattice constant of the nth groove and θ is corresponding diffraction angle. For constructive diffractions, rays from two neighbor grooves should have a phase change of $\Delta\phi = \phi_n - \phi_{n-1} = k_0 b \sin\theta$ that also equals to $(k_{\mathrm{spp}} - G)b$ as the SPP is modulated by the grating, where $G = 2\pi/b$ is the reciprocal vector determined by the local lattice. So, we have the equation of $k_0 b \sin\theta = k_{\mathrm{spp}} b - 2\pi$, which establish a relation between the diffraction angle

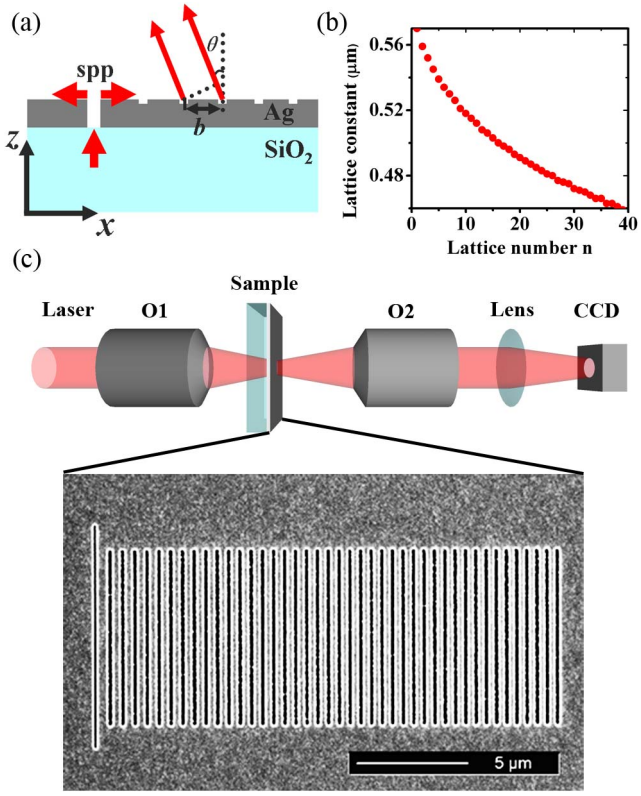

Fig. 1. (a) Schematic diagram of the diffraction principle in our proposed slit-groove structure fabricated on a metal surface. (b) Designed local lattice constants of the surface grooves. (c) Illustration of the experimental setup. Inset is the top-view focus ion beam (FIB) image of the slit-groove structure.

and local lattice. This means every neighboring groove should have an additional phase difference of 2π with respect to all the constructive diffraction beams. Then the phase evolution of the nth groove can be deduced as $\phi_n(x) = \phi_0 + k_{spp}x - 2n\pi$, where ϕ_0 is the initial phase and x is the distance of the nth groove from the initial slit. With a carefully designed grating, a desired diffracted beam in free space with arbitrary phase evolution is accessible. Here, grating with a 1.5-power phase distribution is designed to construct an Airy-shaped radiation beam. According to the scheme of Fig. 1(a), a silver film with the thickness of 100 nm is deposited on a quartz substrate. A single slit with the width of 100 nm (about $\lambda/6$) and a series of grooves with a width of 200 nm, depth of 10 nm, and graded distance on the right side of the slit are fabricated on the metal film. An x polarized light (TM) is normally incident into the slit from the substrate side to launch SPP wave on the air/silver interface. According to the required phase distribution, we can exactly calculate every location of the grooves on the film surface by solving $\phi_n(x) = \Psi(x)$. Here

$$\psi(x) = -\frac{2}{3}\left(\frac{x}{a}\right)^{1.5} - \frac{\pi}{4} \tag{1}$$

is the approximated phase distribution of Airy beam defined by the Airy function of

$$\mathrm{Ai}(x) \cong (-\pi^2|x|)^{-1/4}\sin\left[\frac{2}{3}\left(\frac{|x|}{a}\right)^{1.5} + \frac{\pi}{4}\right] \tag{2}$$

at the start plane of $z = 0$ [16], where $a = 1.21$ μm is a coefficient that determines the acceleration of Airy beams. It is important to note that $\phi_n(x) = \phi_0 + k_{spp}x - 2n\pi$ is for SPPs as the initial phase in the $z = 0$ plane, while $\psi(x)$ is for the one in free space. The calculated local lattice parameter (b) is plotted in Fig. 1(b) and corresponds to the λ_{spp} of 610 nm (with respect to the He–Ne laser $\lambda_0 = 632.8$ nm). In addition to the phase modulation, the Airy function requires an $(x)^{-1/4}$ amplitude distribution, which happens to be fulfilled approximately by the decaying SPP field intensity in propagation.

In the experiment, well-designed groove structure was fabricated by a focused ion beam (Strata FIB 201, FEI Company) on a silver film sputtered on a quartz substrate. The optical setup for measurement is sketched in Fig. 1(c). The inset shows the focus ion beam (FIB) image of the fabricated sample, where 40 grooves with a total length of about 20 μm are fabricated on the right side of the slit. A Gaussian beam from an He–Ne laser (632.8 nm) is normally incident in the slit from the substrate side focused by a microscope objective (O1, 50×, NA of 0.55). The polarization of the laser is perpendicular to the slit to launch SPPs efficiently. The transmitted and diffracted light is then collected by another micro-objective (O2, 100×, NA of 0.93), and finally imaged by a CCD camera. By adjusting the image objective (O2) along the z direction with a high precision translation stage, we get the cross-section images of the beams in x–y plane at different distances (z) from the sample. Figures 2(a)–2(d) show the field distribution at $z = 30$, 20, 10, and 0 μm, respectively. At the $z = 0$ μm plane, a series of beam

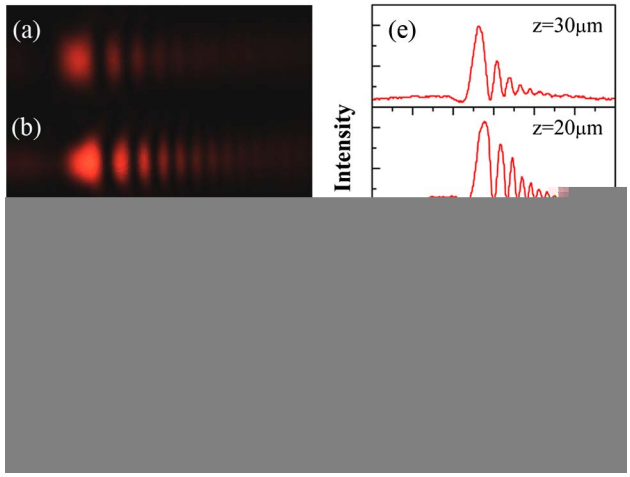

Fig. 2. Measured cross-section images of the transmitted beam in x–y plane at different distances. (a)–(d) with $z = 30$, 20, 10, and 0 μm, respectively. (e) The corresponding intensity profiles.

lobes are constructed at the right side of the slit, which is analog to the cross-section intensity of Airy beam. Figure 2(e) plots the normalized intensity along the symmetric axis of the left images, showing clear multilobe features. As z increases, the beam lobes evidently bend to the left gradually.

To demonstrate the characteristics of the achieved beam more visually, the beam cross-section in x–z plane is depicted in Fig. 3(a) by picking up the intensity along the symmetric axis of the field distribution at x–y planes at a step length of 1 μm along the z axis. The self-bending and nonspreading properties are clearly manifested. A propagation distance of ~50 μm is achieved for the main lobe and its narrow linewidth is well preserved. It should be noted that the dispersive part of beam in the left side of the initial slit [see Fig. 3(a)] indeed attributes to the directly transmitted radiation through the nanoslit. It additionally provides us an intuitive comparison of the generated Airy-like beam and the dispersive transmission where the former reveals much longer propagation distance. The bending trajectory as shown in Fig. 3(b) is further compared with the theoretical parabolic trajectory ($x = z^2/(4k^2a^3)$). A little discrepancy is observed, which would attribute to the paraxial approximation as well as previous reports [17]. The FWHM of the main lobe is also

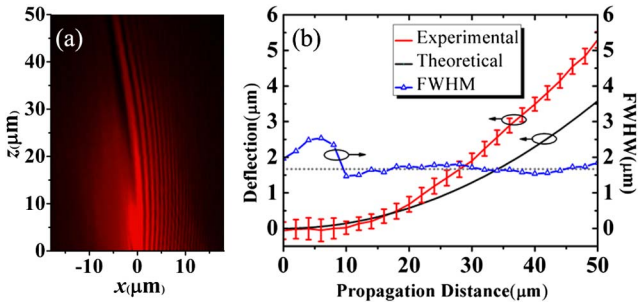

Fig. 3. (a) Retrieved field distribution in x–y plane. (b) Measured trajectory (red with error bar) of the main lobe compared with the calculated parabolic curve (black). The FWHM of the main lobe relative to the propagation distance (blue line) shows an average beam width of ~1.6 μm (dotted gray line).

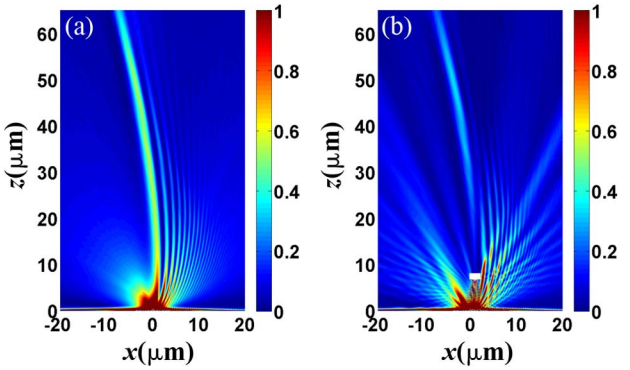

Fig. 4. (a) Simulated intensity distribution of the E field. (b) Self-healing property as a rectangular obstacle (0.8 μm× 0.5 μm, white rectangle) is introduced on the path of the main lobe.

recorded, indicating a small beam width of ~1.6 μm over a long propagation distance of at least 50 μm.

To verify the accelerating beam generation process as well as to explore its self-healing property, numerical simulations using commercial software (Lumerical FDTD Solutions) were performed. The index of the substrate is set to be 1.5 and the permittivity of silver is $\varepsilon_m = -15.93 + 2i$ at the operating wavelength of 633 nm from the Lumerical database with a larger loss. The parameters of the slit and grooves follow the design in the experiment above and a Gaussian beam of 633 nm with x-polarization is incident in the slit from quartz substrate. Figure 4(a) shows the simulated intensity distribution of the electric field at x–z plane, in which the multilobe profile and self-bending property are clearly manifested, agreeing considerably with the experimental results. In addition, a rectangular obstacle (0.8 μm × 0.5 μm) is introduced at $z = 7$ μm to block the main lobe. It is evident that the main lobe reconstructs itself after the obstacle as shown in Fig. 4(b) (the white rectangle represents the obstacle), revealing the self-healing property. As for the fact that the beam lobes are not perfectly maintained in propagation (especially in areas near $z = 0$), it would possibly attribute the monotone phase we designed with $\mathrm{Exp}(i\psi)$ but not the exact $\mathrm{Sin}(\psi)$ as required in the Airy function.

Thus, we have demonstrated that the optical accelerating beam with Airy-like properties can be generated by converting propagating SPP waves to free space radiation with well-designed grooves. It is no doubt that other spatial beams can also be generated flexibly by this method (e.g., a focusing beam). It means that the periodic nanostructures (commonly used to act merely as couplers between the surface wave as well as some guided wave and radiation wave) can be developed to nonperiodic ones with greatly enhanced functionality in beam engineering. Since the SPP beam would have versatile forms, the conversion beams in free space and the manipulations would be fruitful. In this regard, our results bridge the gap of a well-engineered beam between the near field and far field.

In conclusion, we have successfully achieved a spatial accelerating beam with Airy-like profile in the microscale by converting an SPP wave to free space with a well-designed groove grating on a metal surface. The generated beam exhibits self-bending, nonspreading, and self-healing properties. Remarkably, the phase modulation method shows great flexibility from in-plane to out-of-plane. Our results not only promote the diffraction method in beam engineering. They also provide a link between the surface wave and radiation wave in a highly controllable way, which would possibly open an avenue in designing and developing new kinds of micro/nano optical elements and devices.

This work is supported by the State Key Program for Basic Research of China (Nos. 2010CB630703, 2012CB921502, and 2012CB921501), the National Natural Science Foundation of China (Nos. 11174136, 11174128, and 11021403), and PAPD of Jiangsu Higher Education Institutions.

References

1. H. J. Lezec, A. Degiron, E. Devaux, R. A. Linke, L. Martin-Moreno, F. J. Garcia-Vidal, and T. W. Ebbesen, Science **297**, 820 (2002).
2. S. Kim, Y. Lim, H. Kim, J. Park, and B. Lee, Appl. Phys. Lett. **92**, 013103 (2008).
3. N. Yu, J. Fan, Q. J. Wang, C. Pflugl, L. Diehl, T. Edamura, M. Yamanishi, H. Kan, and F. Capasso, Nat. Photonics **2**, 564 (2008).
4. P. Genevet, J. Lin, M. A. Kats, and F. Capasso, Nat. Commun. **3**, 1278 (2012).
5. Y.-H. Chen, L. Huang, L. Gan, and Z.-Y. Li, Light Sci. Appl. **1**, e26 (2012).
6. L. Li, T. Li, S. M. Wang, C. Zhang, and S. N. Zhu, Phys. Rev. Lett. **107**, 126804 (2011).
7. L. Li, T. Li, S. M. Wang, S. N. Zhu, and X. Zhang, Nano Lett. **11**, 4357 (2011).
8. L. Li, T. Li, S. M. Wang, and S. N. Zhu, Opt. Lett. **37**, 5091 (2012).
9. G. A. Siviloglou, J. Broky, A. Dogariu, and D. N. Christodoulides, Phys. Rev. Lett. **99**, 213901 (2007).
10. G. A. Siviloglou and D. N. Christodoulides, Opt. Lett. **32**, 979 (2007).
11. G. A. Siviloglou, J. Broky, A. Dogariu, and D. N. Christodoulides, Opt. Lett. **33**, 207 (2008).
12. J. Baumgartl, M. Mazilu, and K. Dholakia, Nat. Photonics **2**, 675 (2008).
13. I. Kaminer, R. Bekenstein, J. Nemirovsky, and M. Segev, Phys. Rev. Lett. **108**, 163901 (2012).
14. P. Zhang, Y. Hu, T. C. Li, D. Cannan, X. B. Yin, R. Morandotti, Z. G. Chen, and X. Zhang, Phys. Rev. Lett. **109**, 193901 (2012).
15. I. Dolev, I. Epstein, and A. Aire, Phys. Rev. Lett. **109**, 203903 (2012).
16. D. M. Cottrell, J. A. Davis, and T. M. Hazard, Opt. Lett. **34**, 2634 (2009).
17. A. Minovich, A. E. Klein, N. Janunts, T. Pertsch, D. N. Neshev, and Y. S. Kivshar, Phys. Rev. Lett. **107**, 116802 (2011).